Non-linear MHD simulations of ELMs in ASDEX Upgrade

and

JOREK developments for VDE and disruption simulations

Matthias Hölzl
(IPP Garching)

Overview

- Non-linear MHD code
- Bezier finite elements
- Fully implicit time-evolution
- Divertor tokamaks including X-point(s)
- Originally developed at CEA Cadarache

  Czarny and Huysmans (2008); Huysmans and Czarny (2007)
- Reduced MHD in toroidal geometry (next slide)
- Other models:
  - Two-fluid extensions (M. Becoulet, S. Pamela)
  - Neutrals (C. Reux)
  - Full MHD
- Fortran 90/95
- MPI + OpenMP hybrid parallelization

Reduced MHD Equations

$$\frac{\partial \Psi}{\partial t} = \eta j - R\,[u, \Psi] - F_0 \frac{\partial u}{\partial \phi}$$

$$\frac{\partial \rho}{\partial t} = -\nabla \cdot (\rho \mathbf{v}) + \nabla \cdot (D_\perp \nabla_\perp \rho) + S_\rho$$

$$\frac{\partial (\rho T)}{\partial t} = -\mathbf{v} \cdot \nabla(\rho T) - \gamma \rho T \nabla \cdot \mathbf{v} + \nabla \cdot \left(K_\perp \nabla_\perp T + K_{||} \nabla_{||} T\right) + S_T$$

$$\mathbf{e}_\phi \cdot \nabla \times \left\{ \rho \frac{\partial \mathbf{v}}{\partial t} = -\rho(\mathbf{v} \cdot \nabla)\mathbf{v} - \nabla p + \mathbf{j} \times \mathbf{B} + \mu \Delta \mathbf{v} \right\}$$

$$\mathbf{B} \cdot \left\{ \rho \frac{\partial \mathbf{v}}{\partial t} = -\rho(\mathbf{v} \cdot \nabla)\mathbf{v} - \nabla p + \mathbf{j} \times \mathbf{B} + \mu \Delta \mathbf{v} \right\}$$

$$j \equiv -j_\phi = \Delta^* \Psi$$

$$\omega \equiv -\omega_\phi = \nabla^2_{pol}\, u$$

Variables: Ψ, u, j, ω, ρ, T, $v_{||}$

Ideal wall + Bohm boundary conditions

Definitions: $\mathbf{B} = \frac{F_0}{R}\mathbf{e}_\phi + \frac{1}{R}\nabla\Psi \times \mathbf{e}_\phi$ and $\mathbf{v} = -R\nabla u \times \mathbf{e}_\phi + v_{||}\mathbf{B}$

Typical code run

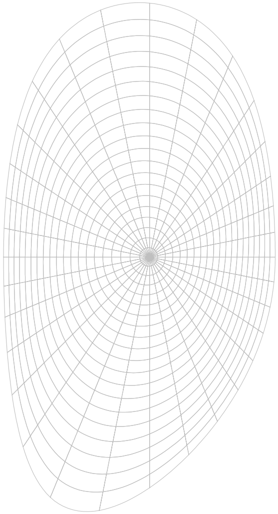

- Initial grid (Grids shown with reduced resolution)
- Equilibrium data (F_0, Ψ_{bnd}, profiles for T, ρ, FF')
- Grad-Shafranov
- Flux aligned grid including X-point(s)
- Radial and poloidal grid meshing
- Grad-Shafranov
- Axisymmetric flows
- Time-integration
- Analysis of restart-files:
    - Poincare plots
    - 2D or 3D VTK files
    - ...

Typical code run

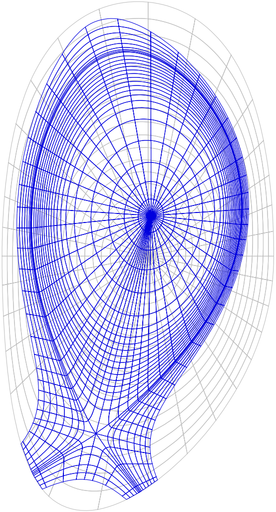

- Initial grid (Grids shown with reduced resolution)
- Equilibrium data (F_0, Ψ_{bnd}, profiles for T, ρ, FF')
- Grad-Shafranov
- Flux aligned grid including X-point(s)
- Radial and poloidal grid meshing
- Grad-Shafranov
- Axisymmetric flows
- Time-integration
- Analysis of restart-files:
  - Poincare plots
  - 2D or 3D VTK files
  - ...

Typical code run

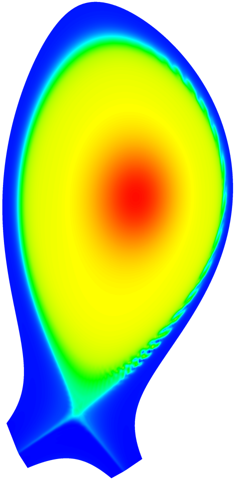

- Initial grid (Grids shown with reduced resolution)
- Equilibrium data (F_0, Ψ_{bnd}, profiles for T, ρ, FF')
- Grad-Shafranov
- Flux aligned grid including X-point(s)
- Radial and poloidal grid meshing
- Grad-Shafranov
- Axisymmetric flows
- Time-integration
- Analysis of restart-files:
  - Poincare plots
  - 2D or 3D VTK files
  - ...

Overview

- ELMs in typical ASDEX Upgrade H-mode equilibrium
- Many toroidal harmonics, resistivity and viscosity too large
- Focus on early phase until non-linear saturation starts

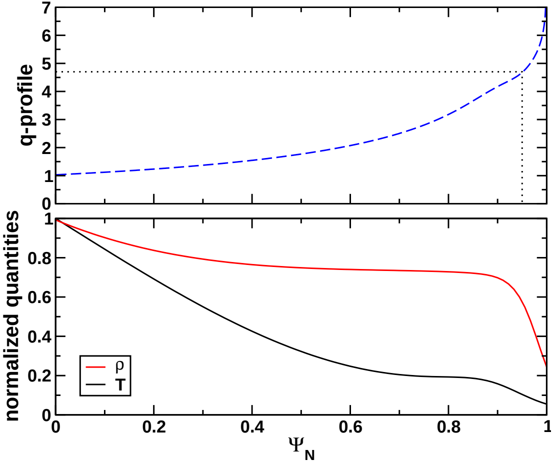

Ballooning Structure

- Mode-coupling causes localization of ballooning-filaments:

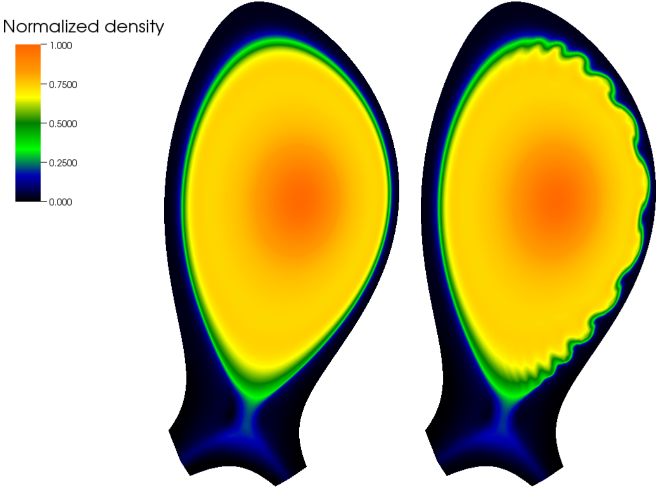

unperturbed $\qquad$ $n = 0, 8, 16$

Ballooning Structure

- Mode-coupling causes localization of ballooning-filaments:

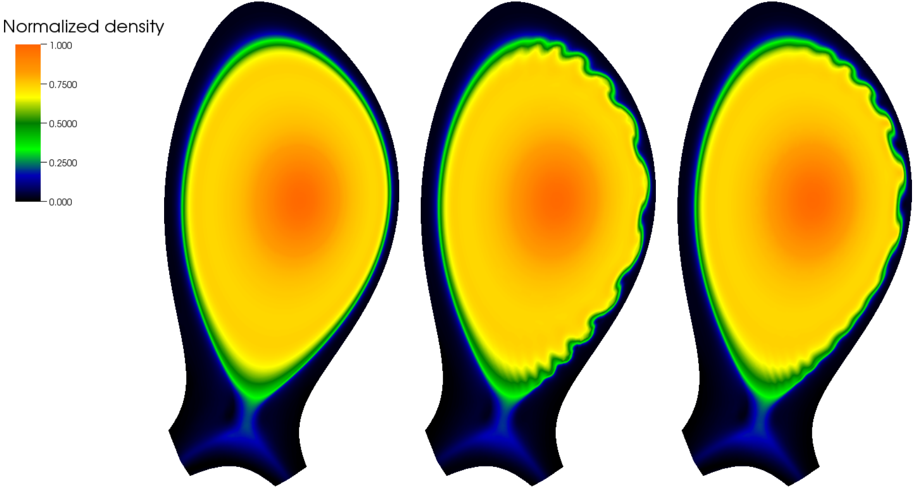

unperturbed | $n = 0, 8, 16$ | $n = 0, 1, 2, \ldots, 16$

Poloidal Flux Perturbation

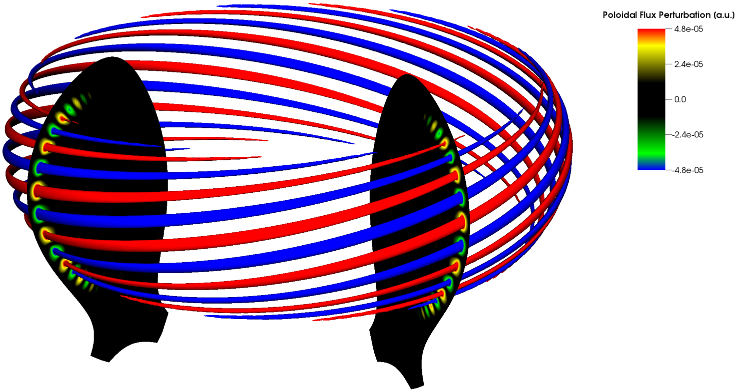

$n = 0, 8, 16$

- Red/blue surfaces correspond to 70 percent of maximum/minimum values

Poloidal Flux Perturbation

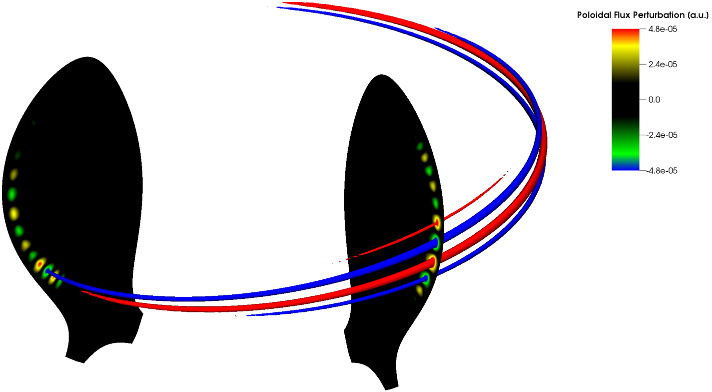

$n = 0, 1, 2, 3, 4, \ldots, 16$

- Red/blue surfaces correspond to 70 percent of maximum/minimum values
- Localized due to several strong harmonics with adjacent n

Solitary Magnetic Perturbation

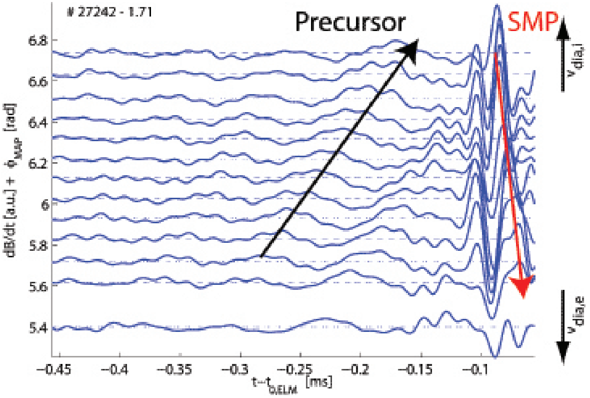

- Solitary Magnetic Perturbation in ASDEX Upgrade Wenninger et al. (2012)
- Distribution of "Solitariness"

Position of Perturbations

- Radial perturbation positions differ between variables

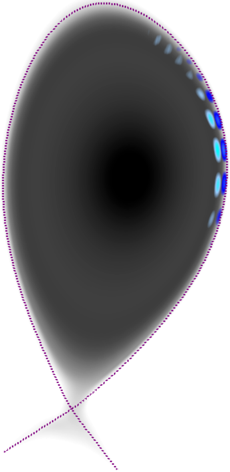

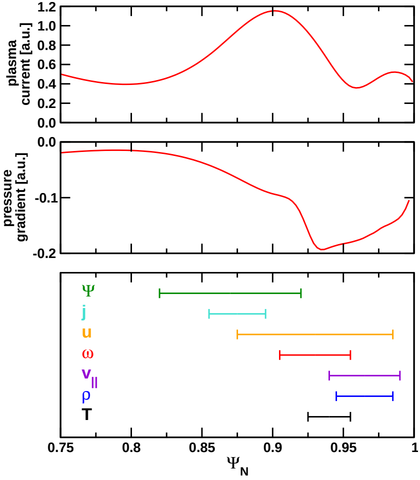

Energy Timetraces

- $n = 1$ (and others) driven non-linearly to large amplitude
  (Subdominant modes not shown for clarity)

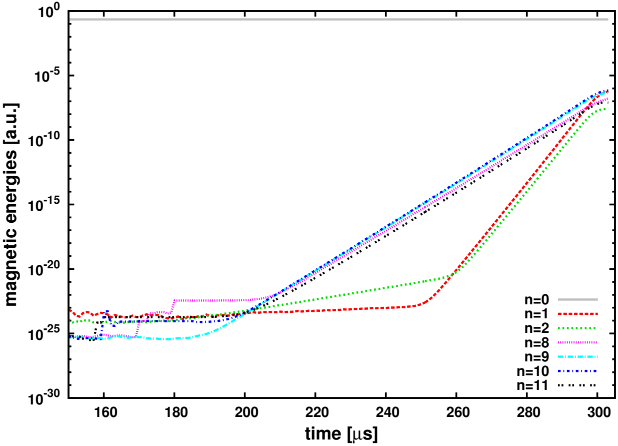

Mode Interaction

- Consider a case with $n = 0, 4, 8, 12, 16$ for the start
- Can we reproduce and understand this with a simple model?

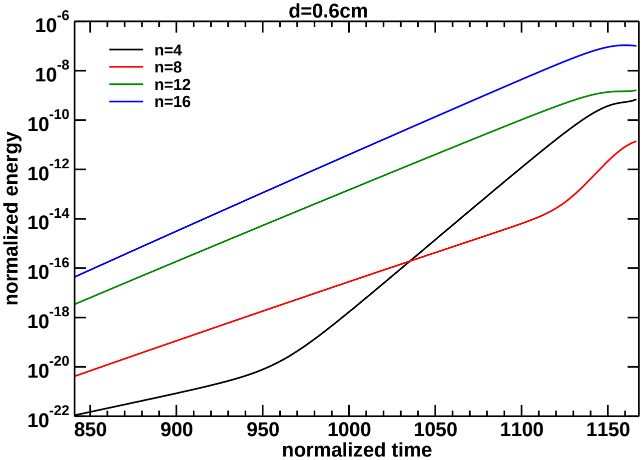

Mode Interaction (2)

- Non-linear terms lead to mixing of toroidal modes
- Quadratic: $(n_1, n_2) \leftrightarrow n_1 \pm n_2$
- For instance: $(8, 4)$, $(12, 8)$, and $(16, 12)$ couple to $n = 4$
- Simple model (Mode rigidity, $n = 0$ fixed):

$$\dot{A}_4 = \overbrace{\gamma_4 \; A_4}^{\text{linear}} + \overbrace{\gamma_{8,-4} \; A_8 \; A_4 + \gamma_{12,-8} \; A_{12} \; A_8 + \gamma_{16,-12} \; A_{16} \; A_{12}}^{\text{non-linear interaction}}$$

Mode Interaction (2)

- Non-linear terms lead to mixing of toroidal modes
- Quadratic: $(n_1, n_2) \leftrightarrow n_1 \pm n_2$
- For instance: $(8,4)$, $(12,8)$, and $(16,12)$ couple to $n = 4$
- Simple model (Mode rigidity, $n = 0$ fixed):

$$\dot{A}_4 = \overbrace{\gamma_4 \; A_4}^{\text{linear}} + \overbrace{\gamma_{8,-4} \; A_8 \; A_4 + \gamma_{12,-8} \; A_{12} \; A_8 + \gamma_{16,-12} \; A_{16} \; A_{12}}^{\text{non-linear interaction}}$$

$$\dot{A}_8 = \gamma_8 \; A_8 + \gamma_{4,4} A_4 \; A_4 + \gamma_{12,-4} A_{12} \; A_4 + \gamma_{16,-8} \; A_{16} \; A_8$$

$$\dot{A}_{12} = \gamma_{12} \; A_{12} + \gamma_{4,8} \; A_4 \; A_8 + \gamma_{16,-4} \; A_{16} \; A_4$$

$$\dot{A}_{16} = \gamma_{16} \; A_{16} + \gamma_{8,8} \; A_8 \; A_8 + \gamma_{4,12} \; A_4 \; A_{12}$$

- Linear growth rates taken from JOREK simulation
- Energy conservation $\Rightarrow$ Six remaining free parameters $\gamma_{i,j}$
- Determine free parameters numerically by minimizing quadratic difference

Mode Interaction (3)

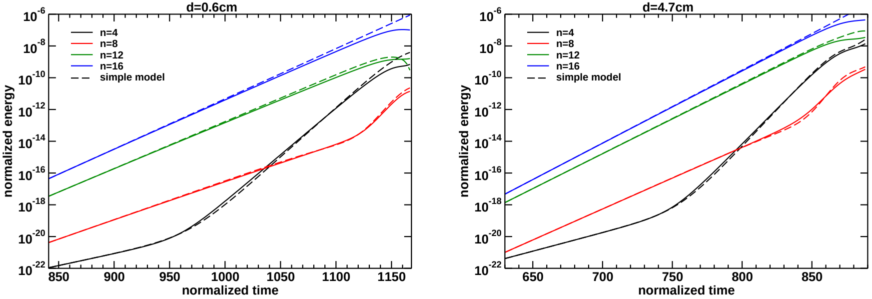

- Saturation not covered by the model (of course)
- Same set of interaction-parameters $\gamma_{i,j}$ for both wall-distances
- Non-linear growth described well
- Same mechanism brings up $n = 1$ in the simulations shown before with poloidally and toroidally localized ELMs!

Overview

- Plasma instabilities interact with conducting structures via eddy currents
- For instance: External kink ($\sim \mu s$) $\rightarrow$ Resistive wall mode ($\sim ms$)
- Aim: Non-linear resistive wall simulations
- Coupling of JOREK and STARWALL codes
- Showing status of (ongoing) implementation and benchmarking

Natural boundary condition

- Current definition equation $j = \Delta^* \Psi$ in weak form (test function v^*):

$$\int dV \, \frac{v^*}{R^2} \, j - \int dV \, v^* \, \nabla \cdot \left(\frac{1}{R^2} \nabla \Psi \right) = 0$$

- Partial integration:

$$\int dV \, \frac{v^*}{R^2} \, j + \int dV \, \frac{1}{R^2} \, \nabla v^* \cdot \nabla \Psi - \oint dA \, \frac{v^*}{R} \, \underbrace{(\nabla \Psi \cdot \hat{\mathbf{n}}/R)}_{\equiv B_{\mathtt{tan}}} = 0.$$

- Ideal-wall boundary conditions: Boundary integral vanishes in “old” JOREK
- Natural boundary condition: Replace $B_{\mathtt{tan}}$ by STARWALL response

Resistive Wall STARWALL

- Developed by Peter Merkel (Merkel and Sempf (2006); Strumberger et al. (2011))
- Executed once for a JOREK simulation
- Conducting structures represented by triangles
  (3D structures including holes possible)
- Wall currents described by current potentials Y_k at triangle nodes
- Vacuum field equation solved outside JOREK domain
  (for set of unit Ψ-perturbations corresponding to Bezier DOFs)
- Expression for B_{tan} in terms of Ψ at the interface (response matrices)

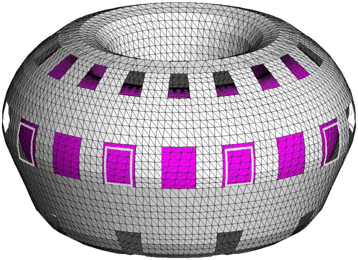

- Ideal wall (algebraic expression):

$$B_{\mathtt{tan}} = \sum_i b_i \sum_j \hat{M}^{\mathsf{id}}_{i,j}\, \Psi_j$$

- Vacuum response: $\hat{M}^{\mathsf{id}}$

- Ideal wall (algebraic expression):

$$B_{tan} = \sum_i b_i \sum_j \hat{M}^{id}_{i,j}\, \Psi_j$$

- Resistive wall:

$$B_{tan} = \sum_i b_i \left(\sum_j \hat{M}^{ee}_{i,j}\, \Psi_j + \sum_k \hat{M}^{ey}_{i,k}\, Y_k \right)$$

$$\dot{Y}_k = -\frac{\eta_w}{d_w}\, \hat{M}^{yy}_{k,k}\, Y_k - \sum_j \hat{M}^{ye}_{k,j}\, \dot{\Psi}_j$$

- Vacuum response: $\hat{M}^{id}$, $\hat{M}^{ee}$, $\hat{M}^{ey}$, $\hat{M}^{ye}$, $\hat{M}^{yy}$
- Discretize consistent with fully-implicit time evolution scheme
- Plug B_{tan} into boundary integral $\oint dA\, \frac{j_i^*}{R}\, \underbrace{(\nabla\Psi \cdot \hat{\mathbf{n}}/R)}_{\equiv B_{tan}}$

Resistive Wall Benchmarks (1)

- Freeboundary equilibrium for ITER-like limiter case: Same boundary-integral
- Allows to test parts (no time-evolution, no wall-currents)
- Flux-surfaces and q-profile agree very well with CEDRES++

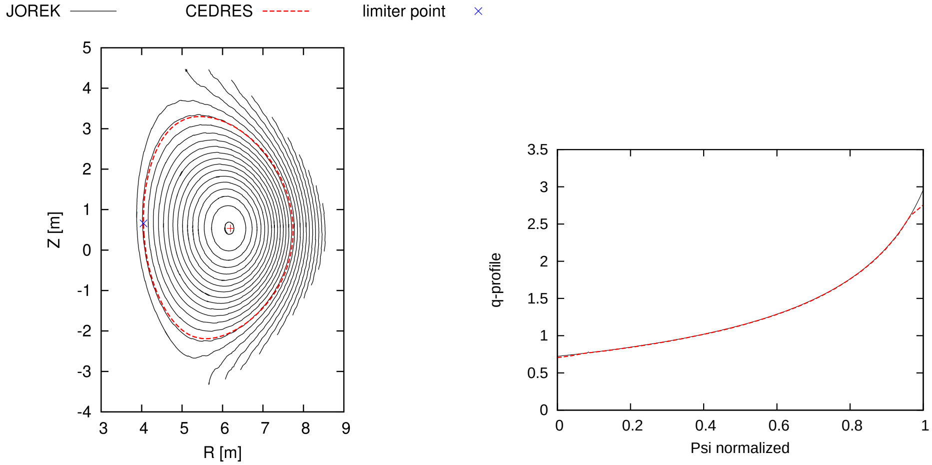

Resistive Wall Benchmarks (2)

- 2/1 tearing mode in circular plasma ($R = 10$, $a = 1$) with ideal wall
- Linear growth rates agree very well with CASTOR

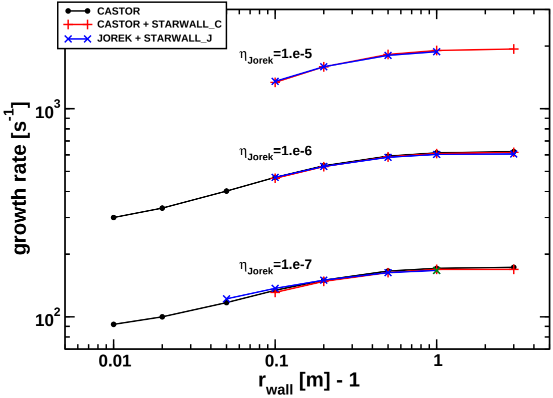

Resistive Wall Benchmarks (3)

- $2/1$ external kink mode in circular plasma with resistive wall
- To be compared to analytical theory and linear simulations (with R. McAdams, I. Chapman)

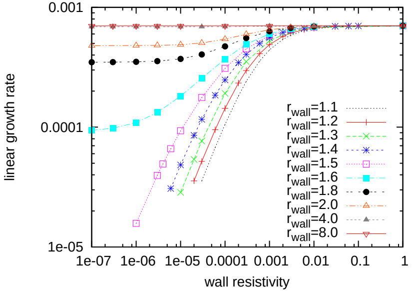

Linear growth rates for different wall radii and wall resistivities

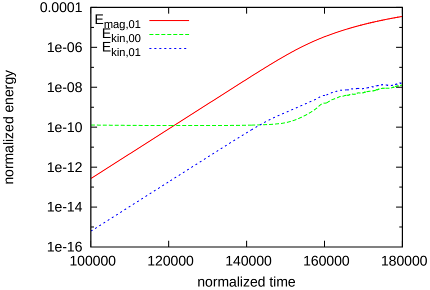

Example for non-linear saturation (stable, small time-steps for convergence)

Resistive Wall Benchmarks (4)

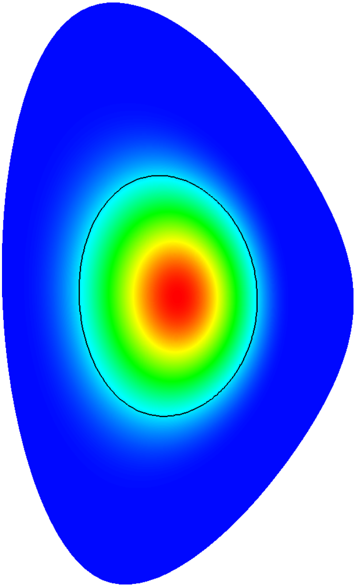

- VDE in ITER-like limiter case
- Preliminary results produced during the last days

Benchmarks (4)

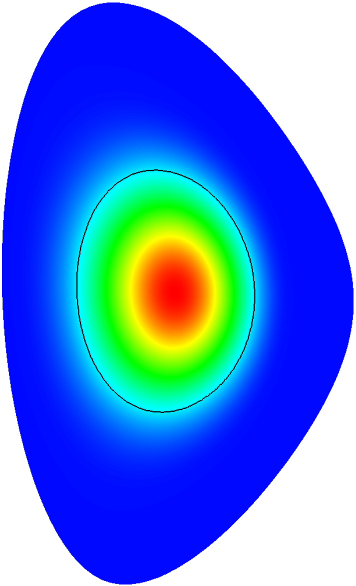

- VDE in ITER-like limiter case
- Preliminary results produced during the last days

Resistive Wall Benchmarks (4)

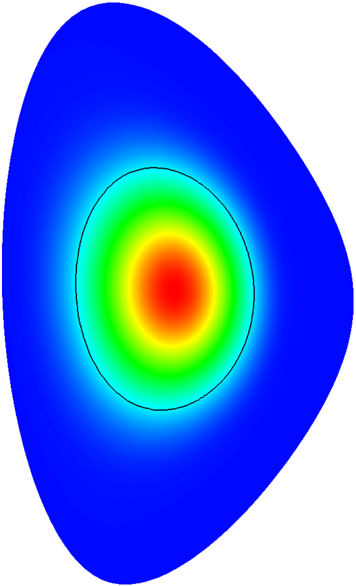

- VDE in ITER-like limiter case
- Preliminary results produced during the last days

Resistive Wall Benchmarks (4)

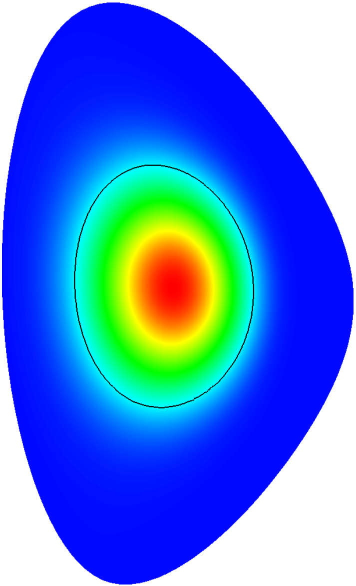

- VDE in ITER-like limiter case
- Preliminary results produced during the last days

Resistive Wall Benchmarks (4)

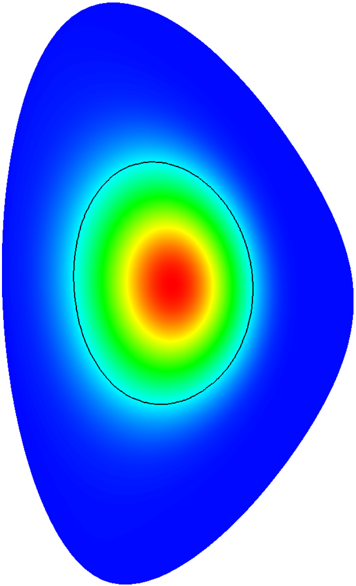

- VDE in ITER-like limiter case
- Preliminary results produced during the last days

Resistive Wall Benchmarks (4)

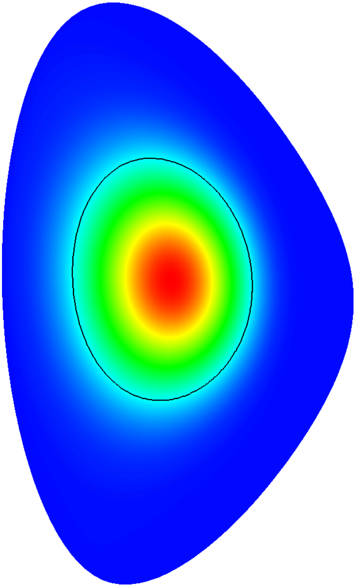

- VDE in ITER-like limiter case
- Preliminary results produced during the last days

Resistive Wall Benchmarks (4)

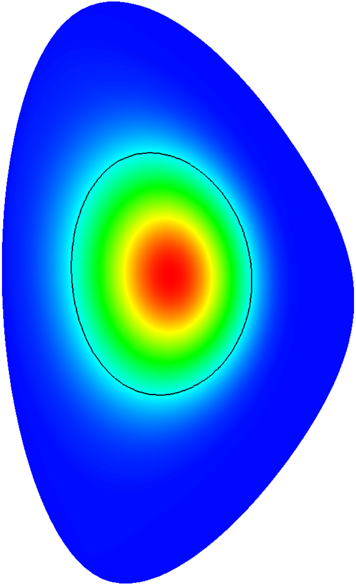

- VDE in ITER-like limiter case
- Preliminary results produced during the last days

Resistive Wall Benchmarks (4)

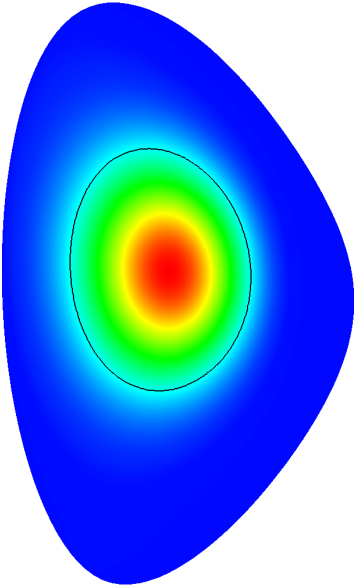

- VDE in ITER-like limiter case
- Preliminary results produced during the last days

Resistive Wall Benchmarks (4)

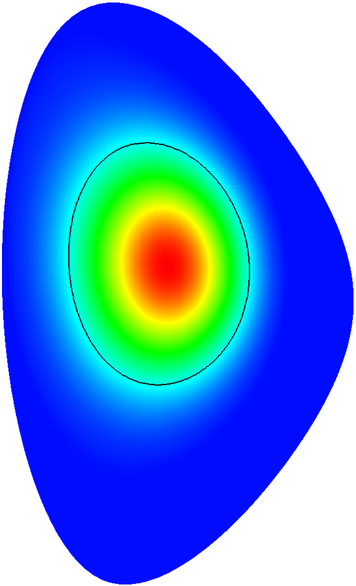

- VDE in ITER-like limiter case
- Preliminary results produced during the last days

Benchmarks (4)

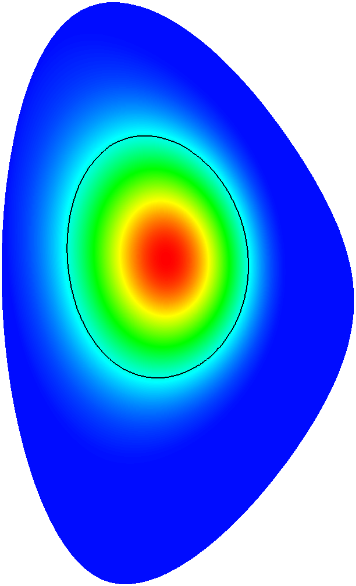

- VDE in ITER-like limiter case
- Preliminary results produced during the last days

Resistive Wall Benchmarks (4)

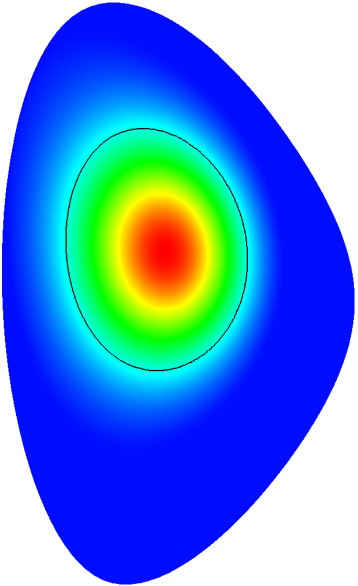

- VDE in ITER-like limiter case
- Preliminary results produced during the last days

Resistive Wall Benchmarks (4)

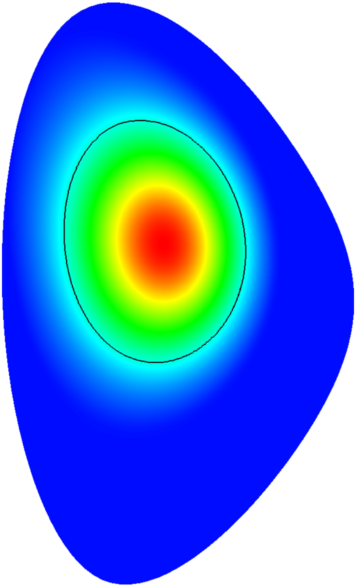

- VDE in ITER-like limiter case
- Preliminary results produced during the last days

Resistive Wall Benchmarks (4)

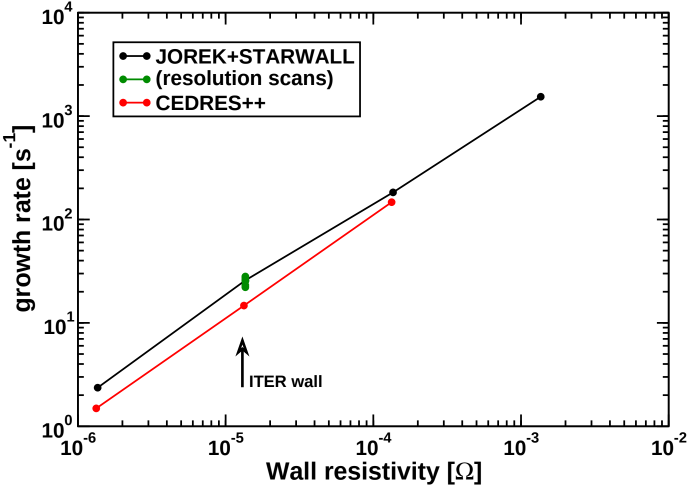

- VDE growth-rates already similar to CEDRES++
- Some numerical issues to be solved
- Improve consistency between equilibrium and time-evolution

Summary

ELM simulations for ASDEX Upgrade

Hölzl et al. (2011, 2012a); Krebs et al. (2013)

- Poloidal and toroidal localization
- Low-n grow non-linearly

→ ELM-types, affected region, heat-flux patterns

→ Interaction with RMPs

Resistive-wall model

Hölzl et al. (2012b)

- Coupling to STARWALL (Merkel and Sempf (2006))
- Ongoing benchmarks look promising

→ Finish implementation and benchmarking

→ Non-linear simulations of RWMs, VDEs, . . .

→ Coil-response, full-MHD, feedback, . . .

References

O. Czarny and G. Huysmans. *Journal of Computational Physics*, 227, 7423 (2008).

M. Hölzl, S. Günter, and ASDEX Upgrade Team. In *Proceedings of the 38th EPS Conference on Plasma Physics*. Strasbourg, France (2011). P2.078.

M. Hölzl, S. Günter, R. P. Wenninger, et al. *Physics of Plasmas*, 19, 082505 (2012a).

M. Hölzl, P. Merkel, G. Huysmans, et al. *Journal of Physics: Conference Series*, 401, 012010 (2012b). doi:10.1088/1742-6596/401/1/012010.

G. Huysmans and O. Czarny. *Nuclear Fusion*, 47, 659 (2007).

I. Krebs, M. Hölzl, K. Lackner, et al. to be published (2013).

P. Merkel and M. Sempf. In *Proceedings of the 21st IAEA Fusion Energy Conference*. Chengdu, China (2006). TH/P3-8.

E. Strumberger, P. Merkel, C. Tichmann, et al. In *Proceedings of the 38th EPS Conference on Plasma Physics*. Strasbourg, France (2011). P5.082.

R. Wenninger, H. Zohm, J. Boom, et al. *Nuclear Fusion*, 42, 114025 (2012).

$\rightarrow$ me.steindaube.de

Acknowledgements

P. Merkel

I. Krebs

G. Huysmans

K. Lackner

S. Günter

E. Nardon

E. Strumberger

Time Discretization

- Discretize consistently with other JOREK equations ($Y_k^{n+1} = Y_k^n + \delta Y_k^n$):

$$(1+\xi)\left[\delta Y_k^n + \sum_j \hat{M}^{ye}_{k,j}\ \delta\Psi_j^n\right] + \Delta t\ \theta\ \frac{\eta_w}{d_w}\ \hat{M}^{yy}_{k,k}\ \delta Y_k^n$$

$$= -\Delta t\ \frac{\eta_w}{d_w}\ \hat{M}^{yy}_{k,k}\ Y_k^n + \xi\left[\delta Y_k^{n-1} + \sum_j \hat{M}^{ye}_{k,j}\ \delta\Psi_j^{n-1}\right]$$

- Crank-Nicholson: ($\theta = 0.5$, $\xi = 0$) or Gears: ($\theta = 1$, $\xi = 0.5$)
- Solve for δY_k^n and insert into $B_{\tt tan}$ at time-step $n+1$:

$$B_{\tt tan}^{n+1} = \sum_i b_i \left[\sum_j \hat{M}^{ee}_{i,j}\cdot\left(\Psi_j^n + \delta\Psi_j^n\right) + \sum_k \hat{M}^{ey}_{i,k}\cdot\left(Y_k^n + \delta Y_k^n\right)\right]$$

- Plug result into boundary integral $\oint dA\ \frac{j_i^*}{R}\ \underbrace{(\nabla\Psi\cdot\hat{\mathbf{n}}/R)}_{\equiv B_{\tt tan}}$

formulation...

$$\sum_{i_{\text{elem}}} \int \frac{dV}{R^2} \left(j_i^* \, \delta j^n + \nabla j_i^* \cdot \nabla \delta \Psi^n \right) - \sum_{i_{\text{bnd}}} \oint dA \, \frac{j_i^*}{R} \sum_i b_i \sum_j \hat{E}_{i,j} \, \delta \Psi_j^n$$

$$= - \sum_{i_{\text{elem}}} \int \frac{dV}{R^2} \left(j_i^* \, j^n + \nabla j_i^* \cdot \nabla \Psi^n \right)$$

$$+ \sum_{i_{\text{bnd}}} \oint dA \, \frac{j_i^*}{R} \sum_i b_i \left[\sum_k \left(\hat{F}_{i,k} \, Y_k^n + \hat{G}_{i,k} \, \delta Y_k^{n-1} \right) + \sum_j \left(\hat{H}_{i,j} \, \Psi_j^n + \hat{J}_{i,j} \, \delta \Psi_j^{n-1} \right) \right]$$

and

$$Y_k^{n+1} = Y_k^n + \sum_j \hat{A}_{k,j} \, \delta \Psi_j^n + \hat{B}_{k,k} \, Y_k^n + \hat{C}_{k,k} \, \delta Y_k^{n-1} + \sum_j \hat{D}_{k,j} \, \delta \Psi_j^{n-1}$$

where

$$\hat{S}_{k,k} = 1 + \xi + \Delta t \theta \, \tfrac{\eta w}{dw} \, \hat{M}^{yy}_{k,k} \qquad \hat{D}_{k,j} = \xi \hat{M}^{ye}_{k,j} / \hat{S}_{k,k} \qquad \hat{H}_{i,j} = \hat{M}^{ee}_{i,j}$$

$$\hat{A}_{k,j} = -(1+\xi) \, \hat{M}^{ye}_{k,j} / \hat{S}_{k,k} \qquad \hat{E}_{i,j} = \hat{M}^{ee}_{i,j} + \textstyle\sum_k \hat{M}^{ey}_{i,k} \, \hat{A}_{k,j} \qquad \hat{J}_{i,j} = \textstyle\sum_k \hat{M}^{ey}_{i,k} \, \hat{D}_{k,j}$$

$$\hat{B}_{k,k} = -\Delta t \, \tfrac{\eta w}{dw} \, \hat{M}^{yy}_{k,k} / \hat{S}_{k,k} \qquad \hat{F}_{i,k} = \hat{M}^{ey}_{i,k} \left(1 + \hat{B}_{k,k} \right)$$

$$\hat{C}_{k,k} = \xi / \hat{S}_{k,k} \qquad \hat{G}_{i,k} = \hat{M}^{ey}_{i,k} \, \hat{C}_{k,k}$$

and

$$\int dV = \sum_{i_{\text{elem}}} \int ds \, dt \, d\phi \, J_2 \, R \qquad \oint dA = \sum_{i_{\text{bnd}}} \int dt \, d\phi \, R \sqrt{\left(\frac{\partial R}{\partial t} \right)^2 + \left(\frac{\partial Z}{\partial t} \right)^2}$$